Arch. Metall. Mater. **70** (2025), 2, 913-920

DOI: https://doi.org/10.24425/amm.2025.153494

M.G. MINCIUNA[1,2], P. VIZUREANU[1,2*], A.V. SANDU[1,2], B. ISTRATE[3]

EVALUATION OF WEAR MECHANISMS OF AN ALUMINUM ALLOY IN EMERGENCY APPLICATIONS

Aluminum-silicon alloys have become a popular choice for applications in the automotive and aerospace industries and have proven themselves through their fault-tolerant processability and respectable static properties at comparatively low costs. Current research has focused on a water jet gun for firefighters. This is an essential device used by firefighters and other emergency response teams to control and direct the flow of water from fire hoses. The role of the research is also to understand the performance of enriched materials in the construction of water guns for firefighters. Through a series of friction and wear tests on aluminum-based alloys, the research establishes correlations between wear performance and the mechanical properties of the materials. These findings provide critical insights into the design and performance of pressure guns, thereby helping to increase the safety and effectiveness of firefighting equipment. The results of the study provide practical recommendations for increasing the durability and functionality of essential firefighting tools.

Keywords: Aluminium; coefficient of friction; scratch test; microhardness

1. Introduction

Aluminum is used in the aerospace industry, in construction, but also in certain emergency equipment where a light and resistant material is needed. The use of aluminum allows the creation of a more radical design and sharper edges, starting from more profiled and more innovative structures [1-2]. Aluminum is used in the form of various alloys, which are characterized both by their low density and excellent mechanical properties [3-5]. Aluminum is valuable in that the parts made of it are almost three times lighter than the steel parts, at an equal resistance [6-8].

It is obvious that only the partial replacement of steel with aluminum would have a huge technical-economic effect [9-11]. For this reason, as well as due to the existence in nature of practically inexhaustible reserves of aluminum, it is rightfully called "the metal of the future" [11-13].

The paper by Zhao et al. [14-16] provides significant insights into the wear behavior of aluminum-silicon alloys under both dry sliding and abrasive conditions. This research contributes to the understanding of how Al-Si alloys can be optimized for industrial applications [17,18]. This study is particularly relevant for applications where friction and wear are major concerns, and it offers valuable data for improving material selection and design in tribological systems.

The paper by Qin et al. [19-21] is a valuable resource for understanding the different wear mechanisms that affect aluminum alloys in industrial applications, offering insights into how alloying elements, microstructure, and surface treatments can mitigate wear. It also emphasizes the importance of selecting the right alloy and treatment based on the specific wear conditions in industrial settings.

The paper by Wang and Zhang [22,23] provides a comprehensive review of the friction and wear behavior of particle-reinforced aluminum matrix composites (AMCs). The paper discusses the dominant wear mechanisms, such as abrasive wear, adhesive wear, and delamination, depending on operating conditions. In industrial applications, these composites are widely used in automotive, aerospace, and electronics sectors where minimizing wear is critical for performance and longevity.

The current research focused on a water discharge gun for firefighters (Fig. 1). This is an essential device used by firefighters and other emergency response teams to control and direct the flow of water from fire hoses. This device is designed to provide more precise control over the water flow and allow the opera-

1 "GHEORGHE ASACHI" TECHNICAL UNIVERSITY OF IASI, FACULTY OF MATERIALS SCIENCE AND ENGINEERING, BLVD. MANGERON, NO. 51, 700050, IASI, ROMANIA
2 ACADEMY OF ROMANIAN SCIENTISTS, 54 SPLAIUL INDEPENDENTEI ST., SECT. 5, 050094 BUCHAREST, ROMANIA
3 "GHEORGHE ASACHI" TECHNICAL UNIVERSITY OF IASI, FACULTY OF MECHANICAL ENGINEERING, BLVD. MANGERON, NO. 51, 700050, IASI, ROMANIA

* Corresponding author: peviz2002@yahoo.com

tor to adjust the pressure and direction of the jet to adequately respond to various intervention scenarios.

The high-capacity water and foam firefighting vehicles are equipped with a p.s.i. type centrifugal pump. 50/8; for determinations; the circuit contains two pipe sections and aluminum water discharge guns.

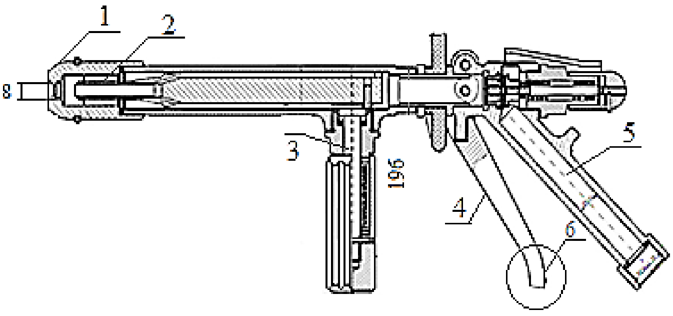

Fig. 1. High pressure water discharge device, TRAPI type (1 spray nozzle; 2 two-start auger; 3 handle; 4 water shut-off valve; 5 quick coupler)

The water discharge gun can be found in special vehicles whose centrifugal pumps also have a high-pressure stage and allows the creation of both the sprayed jet and the compact jet by turning the handle 3, to the left or to the right, in the range 0-180°. To discharge the extinguishing agent, component number 4 must be activated, which has the role of a water shut-off valve. The connection of the pipe to the discharge hose is made through a quick coupler 5, arranged at the terminal part of the pipe. Piece 2 is a two-start auger, which will give the water jet a helical motion. The helical motion of the jet and its collision with the jet passing through the inside of the channel in reference 2 will accentuate the turbulence of the movement in that area, which will cause the jet to break up immediately upon exiting the spray nozzle, element number 1.

2. Materials and methods

The sample subjected to investigations is highlighted in drawing number 6, the water shut-off valve, it is the component on which the greatest resistance is placed because the water pressure is very high (the jets of water pushed over the fire can be compacted or sprayed). In their movement towards the fire, they have to overcome the resistance of the air, especially when it is polluted by smoke and unburnt particles [23-25]. Due to the large difference between the temperature of the fire area and the nearby one, strong air currents are produced that influence the movement of the water jet. The jet trajectory is diverted and reduced, which sometimes makes a direct (precise) attack on the fire source impossible.

Functional characteristics:

- Working fluid: water
- Maximum working pressure: 45 bar
- Maximum diameter: 1.5 m
- Compact jet length: 20±1 m at 40 bar
- Mounting: rubber gaskets; Teflon and polyamide

The performance characteristics (Fig. 2) of a water jet gun are essential to ensure firefighting efficiency, reliability in critical conditions, accuracy and jet control, all contribute to quick and effective interventions, thereby protecting lives and property.

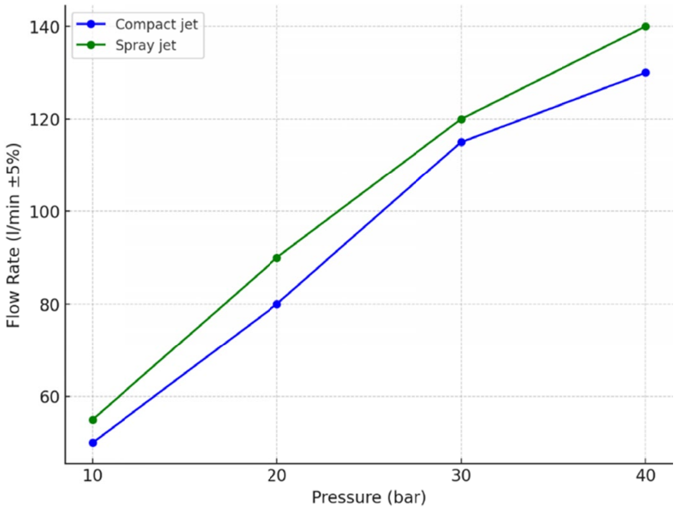

Fig. 2. Flow rate as a function of pressure for compact and spray

After use, the gun is washed with clean water both inside and outside, after which it is wiped with a soft cloth, dried in the open air, then the condition of the connections, gaskets, as well as the normal screwing on the thread of the removable nozzles is checked. Due to emergency interventions, the water pressure gun is not always handled properly, and the surface of the aluminum profiles can be susceptible to scratches, which can affect their appearance. Also, the action of external forces is extremely important, because the so-called internal forces or efforts are created and in these conditions the parts can be deformed [25-27]. Chemical composition determinations were performed on a Foundry Masters type optical spectrometer, model 01J0013, produced by WAS Worldwide Analytical Systems AG using the Al base for analysis. The entire equipment is used to perform quantitative and non-destructive chemical analysis on both semi-finished and finished parts. The analyzed samples were debited, planed and polished on a coarse-grained abrasive paper. The cutting to the dimensions used for the analysis was done with the help of the Metacut M 250 machine, using water jet cooling, in order not to overheat the samples during the cutting operation [28].

For the microscopic examination of the metallographic sample, the alloy was ground, polished and attacked with chemical reagents in order to highlight the structural constituents. A Leica 5000DMI metallographic microscope was used to highlight the structure. The optical micrographs for the Al-Si alloy were made in bright field, at a magnification of 50×, 200×, with the help of the filter: BF – Bright field, which allows obtaining micrographs with a good contrast.

An electron scanning microscope, model Quanta 200 3D dual beam, was used to highlight the structure. The creation of 3D images with the help of SEM and surface data in space is based on the information captured from all angles by the electron detector and based on the penetration depth of the primary electron beam, the configuration of the material in the Z direction can also be reconstructed for a distance of 3-5 µm. The 3D analysis carried out with the help of the scanning electron microscope allows an investigation of surfaces larger than 10-100 µm, a characteristic property of AFM equipment, from the point of view of structural homogeneity, roughness or topographic composition [29-30].

The experimental hardness research was carried out on a PMT3 type microdurimeter, using the Vickers method with a pressing weight of 50 grams. The holding time for each trial was 15 seconds. The term microhardness refers to the static method of hardness determination, using loads that do not exceed 1daN. The diamond penetrator is either the one known from the standard Vickers method, in the form of a pyramid with a square section and an apex angle of 136°, or in the form of an elongated rhombohedral pyramid with an apex angle of 172°30'.

The CETR UMT-2 tribometer was used for determinations of friction forces and static and dynamic friction coefficients on a micro and nanometric scale in rotational motion for various combinations of materials [31-33]. The values for the pressure and friction forces that can be measured are between 0.1 mN and 20 N, with the resolution between 1 µN and 1 mN, depending on the measurement range of the force sensors. The tribometer covers the following force ranges: 0.1 mN÷10 mN, 5 mN÷500 mN and 0.2 N÷20 N.

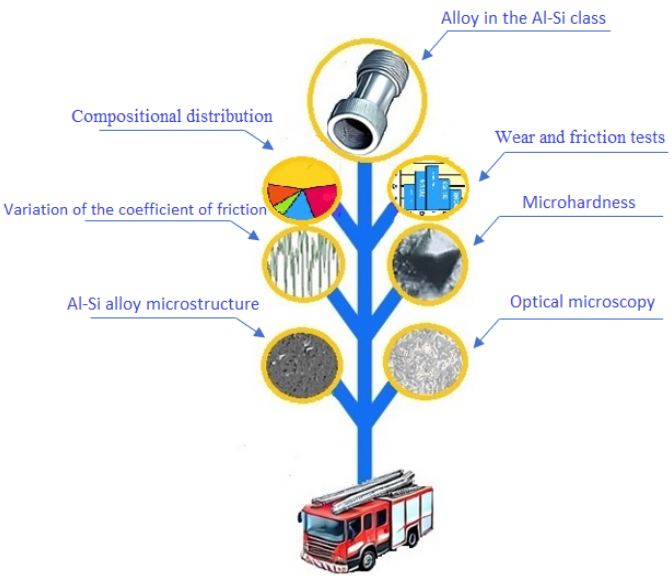

Fig. 3. Overview of the studied alloy

The current study analyzes the behavior of the material in the composition of the water pressure gun using surface analysis, hardness tests and the behavior of the material under the action of external forces with the aim of increasing the device's performance and life span.

3. Chemical characterization of an aluminum-based alloy

Chemical composition determinations were performed on a Foundry Masters type optical spectrometer, using the Al base for analysis.

The analyzed samples were cutting, planed and polished on a coarse-grained abrasive paper.

The cutting to the dimensions used for the analysis was done with the help of the Metacut M 250 machine, using water jet cooling, in order not to overheat the samples during the cutting operation.

TABLE 1

The chemical composition of the alloy

Alloy	Chemical composition [wt.%]							
	Al	Si	Fe	Mn	Mg	Ni	Zn	Other
Guns trapi	94	2.30	0.90	0.60	0.50	0,30	0.20	1.20

The average values determined for the alloying elements, according to the obtained analysis reports, are presented in TABLE 1 and place the analyzed alloy in the Al-Si class.

Alloys of this type are chemically complex alloys. At the same time, they have mechanical characteristics much superior to the standardized ones, resistance to high temperatures, resistance characterized both by minimal expansion and especially by the duration of maintenance at high temperatures when it registers a slow deformation. The alloys also have high toughness. The technological properties of these alloys are determined primarily by the main alloying element, silicon, and on the other hand by the secondary alloying elements that raise certain functional characteristics (Fe, Mg), thus justifying the use of aluminum alloys for the manufacture water jet guns.

4. Microscopic analysis of Al-Si alloy

Fig. 4 shows the optical micrographs for the Al-Si alloy that were made in the bright field, at a magnification of 50×, 200× with the help of the filter: BF – Bright field, which allows obtaining micrographs with a good contrast .

In the case of the Al-Si alloy, the structure is made up of primary silicon crystals and a base mass of coarse α + Si eutectic. Upon solidification of the eutectic, the silicon crystals are deposited at the limit of the α crystals in the form of acicular crystals and negatively influence the mechanical properties.

This disadvantage can be eliminated by thermal treatments, thus obtaining:

- removal and fragmentation of dentritic branches;
- reduction of dentritic grains;
- changing the morphology and shape of the eutectic.

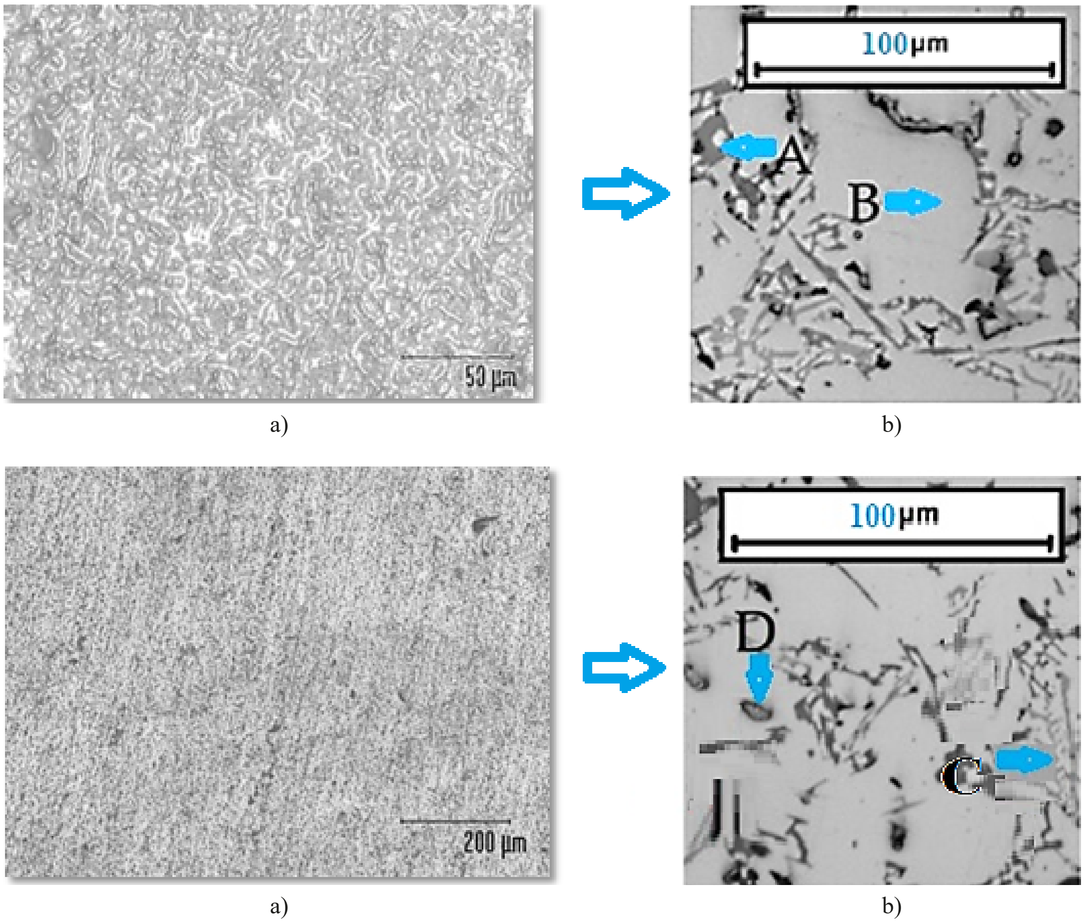

Fig. 4. Optical microscopy images: a) 50×; b) detailed phases; c) 200×; d) detailed phases. A: eutectic Si; B: α-aluminum; C: acicular Fe intermetallic; D: α + Si eutectic

5. Scanning electron microscopic analysis

According to Fig. 5, the Al-Si alloy has a hypoeutectic structure, being composed of α solid solution and fine eutectic. Silumins are characterized by good casting properties, good weldability and high corrosion resistance. The microstructure of these alloys plays a critical role in determining mechanical, thermal and wear performance.

Solidification occurs at a constant temperature, forming a eutectic microstructure consisting of fine silicon (Si) platelets distributed in an aluminum (α – Al) matrix. The eutectic phase is usually responsible for obtaining good casting properties and wear resistance, but must be controlled to avoid embrittlement.

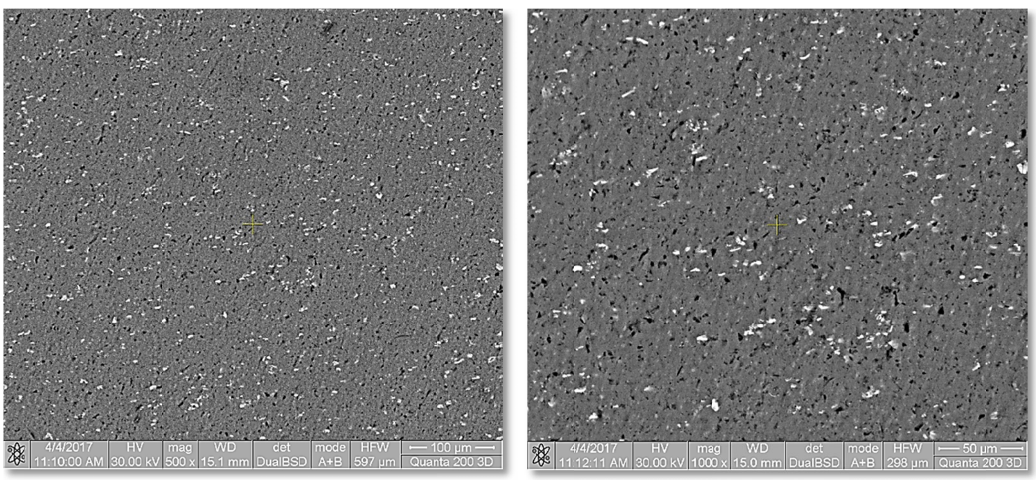

Fig. 5. SEM images of the Al-Si alloy microstructure (500×; 1000×)

6. Microhardness determinations

The microhardness test is used in those cases where "macro" hardness measurement is impossible: materials in the form of thin sheets, very thin layers, determining the hardness of small structural components, measuring the hardness gradient along some directions [28].

The term microhardness refers to the static method of hardness determination, using loads that do not exceed 1daN. The diamond penetrator is either the one known from the standard Vickers method (Fig. 6), in the form of a pyramid with a square section and an apex angle of 136°, or in the form of an elongated rhombohedral pyramid with an apex angle of 172°30'.

Fig. 6. Imprints obtained from microhardness measurements

The experimental measurements were made on a PMT3 type microdurimeter, using the Vickers method with a pressing weight of 50 grams. The holding time for each trial was 15 seconds.

To ensure the accuracy of the results, the samples were subjected to three separate tests, thereby guaranteeing a consistent and reliable evaluation of the materials performance under similar conditions.

TABLE 2

Hardness measurements

Measurement area	Measured point values				Average value
Thickness	HV	69.20	69.10	68.99	**69.09**

The average value obtained (69.09 HV) represents a central measure calculated by summing all the values resulting from the tests and dividing the total by the number of tests, providing a representative estimate of the performance of the samples tested (TABLE 2).

The microhardness values are low, which allows easy machining by chipping and reduced brittleness. The α-Al phase is the softest component of the microstructure. The microhardness values for this phase are relatively low, usually in the range of 40-70 HV (Vickers Hardness). Silicon is much harder than the α-Al phase, having much higher microhardnesses, of the order of 900-1000 HV. In the case of eutectic alloys, silicon wafers have a significant impact on wear behavior and penetration resistance. Primary silicon in hypereutectic alloys shows even higher values of microhardness.

7. The coefficient of friction in dry conditions

Microtribometer allows direct measurement of friction force. In this study, the friction force acts on the elastic lamella of the sensor and is denoted Ff. The data obtained from the force sensor is done with a Vishay P3 tension indicator, and an appropriate software is used to record them. The friction force Ff is determined directly during the experiment, and the coefficient of friction is determined as the ratio of Ff to the normal load G [29-31]. We calibrated the measurement system using loads ranging from 5 mN to 50 mN, the measurement accuracy is 0.2 mN.

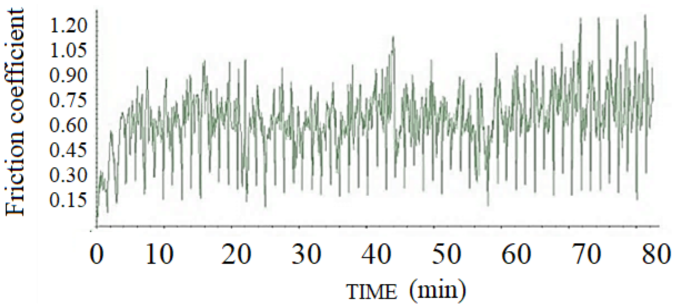

Fig. 7. Variation in relation to time of the friction coefficient

The Fig. 7 shows the variation of the coefficient of friction in relation to time for the sliding speed which has a value of 10 mm/s, steel pin, and the normal load of 10 N. The duration of the experiment was approximately 1 minute, and the coefficient of friction in this interval shows a non-linear variation, a value of 0.15 up to a value of 1.20. The experiment was carried out for one minute, and the obtained results confirm the presence of a non-linear variation starting from a value of 0.15 and reaching 1.20. These results may be due to the probe passing through the smooth and rough zone with a relatively large alternation.

8. Evaluation of mechanical properties through the scratch test

The scratch test following ASTM C 1624 standards (Standard Test Method for Adhesion Strength and Mechanical Failure Modes of Ceramic Coatings by Quantitative Single Point Scratch Testing) is used to assess the adhesion strength of the substrate and identify failure modes within it.

After obtaining *the graph it is possible to collect the data and we can see that* the imprint started to be produced in the

10th second, corresponding to a force of 10 N. It can be observed the large variations of the coefficient of friction from the value of 0.15 to 1.35, these changes being caused by the porosity of the layer.

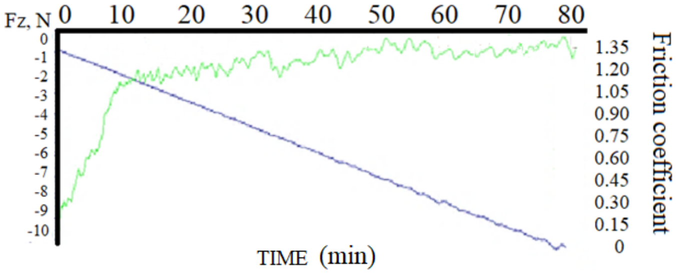

Fig. 8. Evolution of the friction coefficient in relation to the applied force

Following the graph generated during the test by the variation of the coefficient of friction depending on the applied force, three zones were presented (Fig. 9):

I. the starting area (corresponding to the application of a force from 0-3 N),

II. end zone (6-10 N).

The SEM micrographs highlighted the behavior of the Al-Si alloy and confirm that the damage is not visible on the surface.

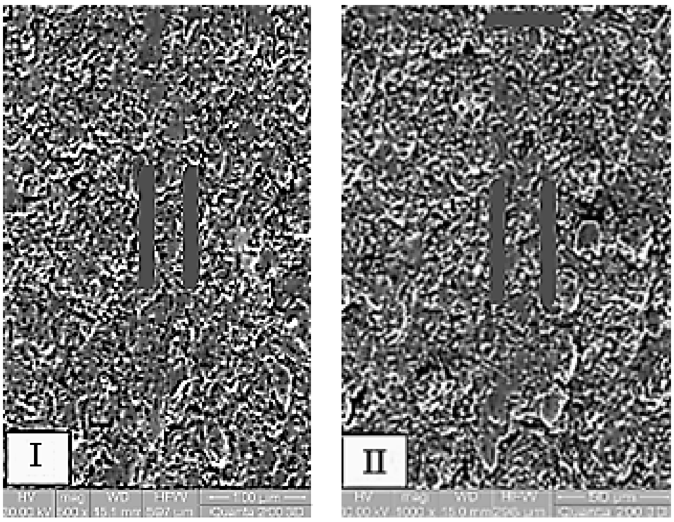

Fig. 9. SEM images of the Al-Si alloy: zone I, b) zone II

In the two images, there are two parallel channels, which are the result of a scratch test (Fig. 7). These channels indicate a process of local plastic deformation of the aluminum matrix and/or the crushing of silicon particles along the scratch path. The surface between and around the scratches shows a rough texture, suggesting the presence of multiple phases, including aluminum and hard silicon particles. This texture could be the result of a combined wear process involving both plastic deformation of the aluminum matrix and mechanical damage to the silicon. The background texture is similar in all three images, but there may be subtle variations in the depth and width of the scratch channel.

9. Discussions

The alloy's performance under typical testing conditions can be usefully gauged by its average microhardness value of 69.09 HV. This value is consistent with usual values for aluminum alloys rich in α-Al and shows that the alloy is in a relatively low hardness range. This alloy's low microhardness values suggest that it is easily machinable, which is a desirable characteristic in applications that call for chipping or cutting to shape and finish. Because low hardness indicates less brittleness, there is less chance of the material chipping or breaking during machining. This property increases the alloy's adaptability, particularly in production procedures requiring precision cutting or complex shapes. Machinability without sacrificing structural integrity is a desirable quality in applications such as industrial fittings or automobile components.

The soft matrix in this alloy's microstructure is the α-Al phase, which typically has microhardness values between 40 and 70 HV. This stage keeps the material from becoming overly brittle by absorbing shocks and offering a certain amount of ductility. α-Al balances the harder, more brittle silicon phases in the structure by allowing the alloy to show some flexibility due to its lower hardness. Because it can aid in stress dissipation and lessen the chance of crack propagation, this softer matrix is also essential in situations where the alloy is subjected to dynamic stresses.

The characterization of a high pressure water discharge device, type TRAPI, is intended to be a step forward in the evolution of advanced alloys. The work includes characterizations of aluminum alloys, especially Al-Si, but also experimental tests regarding chemical, structural and mechanical characterization. Starting from a well-defined current stage, macro and microstructural analyzes and hardness tests highlight the behavior of the alloy and perfectly frame the field of use.

This investigation of microhardness and microstructural phases sheds light on how aluminum alloys balance wear resistance and machinability. While the high hardness of silicon phases greatly enhances wear resistance, the low microhardness of the α-Al phase makes machining easier. Because of this balance, the alloy is adaptable and ideal for uses requiring both moderate hardness and processing ease. Small surface or compositional changes could further optimize the alloy's qualities for applications needing improved performance in wear-intensive environments.

Applying surface treatments or changing the silicon composition (to increase the number of hard phases) may improve performance even further for applications requiring even better wear resistance. As an alternative, alloying with trace amounts of other elements, such as copper or magnesium, could make the aluminum matrix harder, lowering the hardness differential between phases and possibly improving wear characteristics uniformity.

10. Conclusions

The complex characterization of the alloy is highlighted by the wear tests involving several factors: (contact temperature, physical and chemical properties of the materials, contact geometry, etc.).

A sustainable design that does not consider a critical analysis of local effects, wear, and, in some cases, corrosion, can lead to premature and unexpected failures in numerous technical fields. Silicon is the main component for improving fluidity performance, and the best fluidity can be obtained from eutectic to peri-eutectic. However, the crystalline precipitation of silicon tends to form hard spots, which makes machinability poor, generally not allowed to exceed the eutectic point. In addition, silicon improves tensile strength, hardness, machinability and high temperature resistance while reducing elongation.

In conclusion, microhardness in aluminum-silicon alloys is influenced by the composition and microstructure of the material. Silicon contributes to increased hardness, while the aluminum phase provides a balance between hardness and ductility. Controlling the distribution of these phases is essential for optimizing the mechanical properties of these alloys. Due to this property, the use of aluminum alloys for the manufacture of water jet guns is justified. The evolution of the coefficient of friction over time (around 1 minute) shows a non-linear variation, starting from a minimum value of 0.15 and reaching a maximum of 1.20. The variation of the coefficient of friction is explained by the fact that the surface irregularities cause the probe to pass through both smooth and rough areas with a relatively high alternation.

The analysis of the scratch test emphasizes both the resistance to contact pressure and the friction properties. The analyzed alloy demonstrates a high resistance to point contact and a relatively low coefficient of friction.

The scratch test performed on the Al-Si alloy confirms that it is a material with high resistance, thus we can recommend it in the manufacture of parts with direct contact and medium force actuation. The SEM micrographs highlight the malleable properties of aluminum, so the penetrator used in the scratch test created a pressure channel with smooth edges, without adhesion and without microcracks across the entire contact area. The visible roughness and granular structure indicate that the silicon particles resisted scratching to a greater extent than the aluminum matrix, which generated this complex texture. We also propose as a solution the strengthening of alloys by heat treatment, more precisely artificial aging, which involves heating the alloy at a temperature lower than the solubilization temperature (usually in the range of 100-200°C) for several hours, which accelerates the precipitation process hard phases such as Mg_2Si in aluminium-magnesium-silicon alloys. During this process, secondary phase particles (precipitates) form and disperse in the crystal lattice, creating blockages in the movement of dislocations and thus increasing the hardness and strength of the alloy.

REFERENCES

[1] R. Goswami, S. Bhattacharya, Tribological Properties of Aluminium Alloys for Industrial Applications. Elsevier 2023.

[2] R.S. Mishra, Z.Y. Ma, Friction Stir Welding and Processing. Science and Engineering. 3rd Edition, Springer 2022.

[3] J. Fan, X. Li, L. Wang, Effect of Si content on the microstructure and wear behavior of Al-Si alloys under dry sliding conditions. Materials Science and Engineering A **830** (2022).

[4] L. He, H. Huang, Study on the wear mechanism of aluminum alloy in a high-temperature environment. Materials Science and Engineering A **825**, 141963 (2021).

[5] M.I. Hutchings, P. Shipway, Tribology: Friction and Wear of Engineering Materials. 2nd Edition, Butterworth-Heinemann 2017.

[6] P. Ghosh, I. Manna, A study on the wear resistance of aluminum alloys under different loading conditions. Materials Science and Engineering A **790** (2020).

[7] L. Zhao, X. Shi, X. Yan, Tribological properties of Al-Si alloys under dry sliding conditions. Wear **426-427**, 56-62 (2019).

[8] K. Bhanumurthy, G. Naik, Tribological performance of aluminum alloys and composites: A comprehensive review. Materials Today: Proceedings **58**, 1273-1278 (2022).

[9] A. Ahmad, A. Murtaza, A review on the mechanical and tribological behavior of aluminum matrix composites. Journal of Materials Engineering and Performance **29** (6), 3545-3561 (2020).

[10] S. Kumar, R. Mehta, Mechanical properties and wear behavior of aluminum matrix composites for industrial applications: A review. Materials Today: Proceedings **62**, 2045-2051 (2023).

[11] F.M. Moussa, A.A. Masoud, Effects of surface treatment on the wear behavior of aluminum alloys. Journal of Materials Engineering and Performance **29** (4), 2007-2020 (2020).

[12] M. Sunil, P. Aashendra, N. Mrigesh, K. Ajaya, Comparative Study of Microstructure and Properties of Hypoeutectic Al-Si Alloys Being Cast With and Without Melt Thermal Treatment. Metallography, Microstructure, and Analysis **11**, 415-424 (2022).

[13] E. Fracchia, F. Gobber, Effect of Alloying Elements on the Sr Modification of Al-Si Cast Alloys. Metals **11** (2), 342-350 (2021). DOI: https://doi.org/10.3390/met11020342

[14] Y. Zhao, X. Yang, H. Wu, Tribological performance of aluminum-silicon alloys under dry sliding and abrasive conditions. Wear **486**, 204082 (2021).

[15] S. Zhang, Y. Zhang, High-temperature wear resistance of aluminum matrix composites: A review. Journal of Alloys and Compounds **846**, 156203 (2020).

[16] A. Gupta, D. Bhattacharya, Wear and corrosion behavior of aluminum alloys in challenging environments: A review. Corrosion Reviews **40** (1), 55-73 (2022).

[17] ASM International. Properties and Selection: Nonferrous Alloys and Special-Purpose Materials. ASM Handbook **2** (1990).

[18] H. Peng, D. Zhao, Investigation on mechanical and wear properties of novel Al-based composites reinforced with graphene. Materials Characterization **180**, 111406 (2021).

[19] X. Qin, S. Wang, F. Liu, Wear mechanisms of aluminum alloys in industrial applications: A review. Tribology International **148**, 106315 (2020).

[20] S. Kumar, R.K. Sharma, Influence of heat treatment on wear resistance and microstructure of aluminum alloy composites. Journal of Materials Research and Technology **19**, 354-364 (2022).

[21] M.G. Minciuna, P. Vizureanu, Research on the mechanical behavior of some aluminum-based alloys. European Journal of Materials Science and Engineering **6**, 4, 205-211 (2021).

[22] Y. Wang, J. Zhang, A Review of the Friction and Wear Behavior of Particle-Reinforced Aluminum Matrix Composites. Lubricants **11** (8), 317-325 (2023).
DOI: https://doi.org/10.3390/lubricants11080317

[23] Y. Wang, J. Zhang, Effect of alloying elements on the wear behavior of aluminum alloys: A systematic review. Wear **482-483**, 203896 (2021).

[24] J. Singh, A. Chauhan, M. Kumar, A review on wear behavior of aluminum-based metal matrix composites under different testing environments. Materials Today: Proceedings **26** (2), 1628-1632 (2020).

[25] M. Chennakeshavulu, B. Mohan, A review on the effect of microstructural features on wear behavior of aluminum alloys. Materials Science and Engineering A **746**, 30-41 (2019).

[26] P. Sharma, S. Gupta, Wear characteristics of aluminum alloys under extreme loading conditions. Journal of Materials Research and Technology **9** (1), 1157-1169 (2020).

[27] J. Yang, C. Liu, Y. Ma, Tribological performance of aluminum alloys in firefighting equipment: A comprehensive study. Materials Today: Proceedings **21**, 474-478 (2020).

[28] Z. Zhengyu, S. Raja, E. Edwin, A Review on Tribocorrosion Behavior of Aluminum Alloys: From Fundamental Mechanisms to Alloy Design Strategies. Corros. Mater. Degrad. **4** (4), 594-622 (2023). DOI: https://doi.org/10.3390/cmd4040031

[29] P. Babu, S. Karthikeyan, An overview of the wear behavior of aluminum matrix composites and their tribological applications. Journal of Materials Research and Technology **12**, 1563-1582 (2021).

[30] A. Rai, S. Kumar, Microstructural effects on wear performance of aluminum alloys: Insights for design. Materials Science and Engineering: A **786**, 139350 (2020).

[31] A.A. Mohammed, A. Amin, A review of tribological performance of aluminum alloys in aerospace applications: Implications for emergency service. Journal of Materials Research and Technology **14**, 1624-1635 (2021).

[32] A. Mitru, A. Semenescu, G. Simion, E. Scutelnicu, I. Voiculescu, Study on the Weldability of Copper – 304L Stainless Steel Dissimilar Joint Performed by Robotic Gas Tungsten Arc Welding. Materials **15**, 5535 (2022).
DOI: https://doi.org/10.3390/ma15165535

[33] A.V. Sandu, C. Bejinariu, G. Nemtoi, I.G. Sandu. P. Vizureanu, I. Ionita, C. Baciu, New anticorrosion layers obtained by chemical phosphatation. Revista de Chimie **64**, 8, 825-827 (2013).